LAUTECH Journal of Engineering and Technology 18 (2) 2024: 128-137
10.36108/laujet/4202.81.0221

Iron oxide green synthesized nanoparticles for improved performance in monolithic dye-sensitized solar cells

[1,3]Abiodun A. J., [1]Alamu G. A., [1,2*]Adedokun O., [3]Daramola O. O., [1,2]Sanusi Y. K.

[1]*Department of Pure and Applied Physics, Ladoke Akintola University of Technology, P.M.B. 4000, Ogbomoso, Nigeria*
[2]*Nanotechnology Research Group (NANO+), Ladoke Akintola University of Technology, Ogbomoso, Nigeria.*
[3]*Department of Physics, Lead City University Ibadan, Oyo Nigeria*

Article Info

Article history:

Received: May 30, 2024
Revised: June 19, 2024
Accepted: June 25, 2024

Keywords:

Green synthesis; Nanoparticles; Iron oxide; Counter; electrode; Monolithic; Dye-Sensitized Solar; Cell; Conversion efficiency.
.

Corresponding Author:
oadedokun@lautech.edu.ng

ABSTRACT

This study examined the effects of incorporating green-produced iron oxide nanoparticles into a nanoporous carbon counter electrode as a means of improving photovoltaic efficiency in Monolithic Dye-Sensitized Solar Cells (MDSSCs). An extract from the leaves of Ocimum gratissimum was used to synthesize iron oxide nanoparticles. The development of iron oxide nanoparticles was verified by optical absorption in the 350–450 nm range. With an average crystallite size of 47.9 nm, XRD patterns demonstrated the crystalline nature of the Iron oxide nanoparticles. Chemical bonds that may be responsible for the nanoparticle production were found using FTIR investigations. The MDSSC performance evaluation without nanoparticles has a solar-to-electric power conversion efficiency of 1.7%, an open circuit voltage of 0.2625 V, a short-circuit current of 0.0723 mA/cm^2, and a fill factor of 0.3630. MDSSC with FeO nanoparticles has an open-circuit voltage of 0.4274 V, a short-circuit current of 0.1042 mA/cm^2, and a fill factor of 0.46. and solar-to-electric power conversion efficiency of 4.0%. This implies an impressive 135.3% percentage increase in efficiency being recorded for cells containing the iron oxide nanoparticles compared to the cells without NPs. The potential of incorporating green-synthesised iron oxide nanoparticles into MDSSC counter electrodes was shown by their great biocompatibility and even dispersion.

INTRODUCTION

Biosynthesis encompasses various applications, including environmentally friendly manufacturing processes facilitated by nanotechnology, which aim to reduce waste products and enhance a green environment. This involves utilizing nanomaterials as catalysts to enhance the efficiency of current manufacturing methods, thereby minimizing, or eliminating the use of toxic substances. Additionally, nanomaterials and nanodevices are employed to mitigate pollution and improve alternative energy production (Geoffrey *et al.*, 2008). The biosynthesis of nanoparticles adopts a bottom-up approach primarily involving reduction or oxidation reactions. Key reducing agents such as citric acid, ascorbic acid, flavonoids, and enzymes found in microbial and plant extracts play pivotal roles in this process, contributing to both the stabilization and reduction of nanoparticles (Pandey *et al.*, 2012). Green synthesis offers numerous advantages over traditional chemical and physical methods, being cost-effective, environmentally friendly, easily scalable for large-scale production, and requiring no high pressure, energy, temperature, or hazardous chemicals (Ca., 2003). Green synthesis has been gaining so much attention by using various biological resources both as reducing and capping agents (Ahmad *et al.*, 2019). Gulzar et al. (2021)

conducted a study to create zinc oxide nanoparticles (ZnONPs) in a unique, safe, economical, and environmentally friendly manner by using Bergenia ciliate extract as a capping and reducing agent without the use of any hazardous materials (Gulzar *et al.,* 2021). Green nanotechnology-based nanoparticles have also been reported to have some antioxidant and antimicrobial properties (Hossein *et al.,* 2021). However, since dye-sensitized solar cells (DSSCs) offer a low-cost and incredibly effective substitute for traditional inorganic-based solar cells, they are currently the subject of intense scientific and commercial attention. DSSCs consist of a network of interconnected TiO_2 nanoparticles containing dye molecules (Adedokun *et al.,* 2016; O'Regan and Gratzel, 1991). Over the past 20 years, DSSCs have been studied after the findings of the Gratzel and O'Regan study (Chen *et al.*, 2009). It has been noted that DSSC development has accelerated recently (Lee *et al.,* 2012). Furthermore, when it comes to materials and production parameters, DSSCs are more environmentally friendly than conventional photovoltaic systems (Adedokun *et al.,* 2018). Soon, DSSCs will be a desirable renewable power source due to these benefits. Transparent conducting oxide (TCO)-)-coated glass is typically used as the base for DSSC fabrication. This type of structure is known as a "sandwich construction," where the Pt counter electrode is placed on one substrate and the TiO_2 working electrode is applied to the other (Park *et al.,* 2015). One of the priciest parts of DSSCs is the TCO glass. Therefore, the commercial production of DSSCs is particularly challenging due to the use of TCO glass. To overcome the aforementioned difficulty, so-called monolithic designs have been put forth as an alternate framework. Compared to conventional DSSCs, monolithic DSSCs (M-DSSCs) are made on a single TCO substrate, theoretically using half as much TCO. An inorganic spacer layer, a carbon-based counter electrode, and a mesoporous TiO_2 nanocrystal electrode on a transparent fluorine-doped tin oxide (FTO) substrate make up a typical M-DSSC. The working mechanism of a general DSSC is the same. But M-DSSCs are not like regular DSSCs in that the carbon-based materials serve as both the charge conductor and the catalyst for reducing the electrolyte, whereas a Pt-coated TCO substrate would have been the counter electrode utilized to decrease the tri-iodides (Hinsch *et al.,* 2008). The advantages of M-DSSCs include lower costs and an easier production procedure. Their materials and design, however, have not been thoroughly examined for commercialization potential. Since the photoanodes of ordinary DSSCs and M-DSSCs are identical, they must exhibit equivalent cell efficiency. By modifying new materials and device architectures, cell efficiency can still be increased even though carbon-based materials lack the conductivity capacity of marketed TCO/Pt (Ito *et al.,* 2008a; Kay and Gratzel, 1996; Murakami *et al.*, 2006; Ito *et al.*, 2008b).

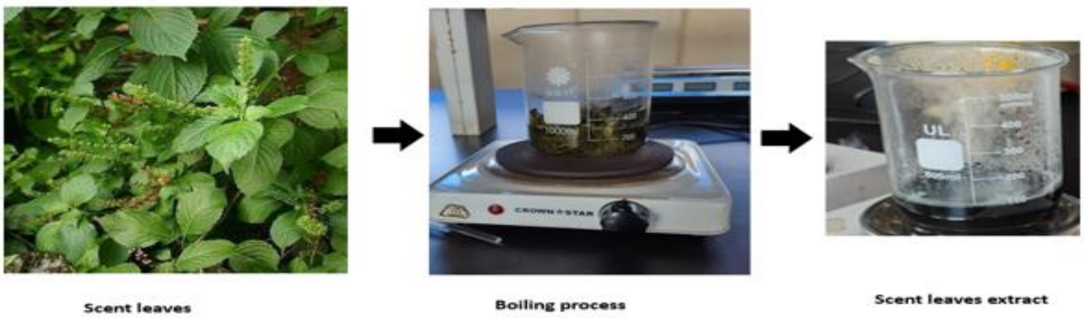

Plate 1.0: Preparation process of the plant extracts

This study introduces green synthesized iron oxide nanoparticles incorporated into the porous carbon combination, which addresses the porosity problem of metal films in monolithic constructions, as well as the low conductivity and fragility associated with carbon electrodes. The iron oxide nanoparticles were tuned and analysed to examine their morphological and structural characteristics. When doped porous carbon is employed in large-scale production instead of platinum, fabrication costs are also reduced. In this study, we used the monolithic approach to fabricate the DSSC and produced an improved porous carbon counter-electrode.

MATERIALS AND METHOD

Materials

Scent leaf (Occimum grattissimum) leaves were obtained from a farm in the Moniya neighbourhood of Ibadan, Oyo state, Nigeria. Solaronix S.A. provided the chlorin e6 dye, fluorine-doped Tin Oxide (FTO) conducting substrates (50 × 50 × 1.1 mm, 10 Ω/sq), and zirconia oxide paste (ZrO2). Analytical grades of titanium dioxide and iron nitrate obtained from Sigma-Aldrich were utilized without undergoing additional purification.

Green synthesis of iron oxide nanoparticles

Freshly picked Occimum grattissimum leaves were air-dried, cleaned in deionized water, and separately milled into a fine powder. As indicated in Plate 1.0, 100 g of the dried fine powder was boiled for 30 minutes in 500 ml of distilled water in a 1000 ml flask. The extract was then filtered through Whatman no. 1 filter papers.

Occimum grattissimum leaf extract in aqueous form was used to produce FeO, acting as a capping and reducing agent simultaneously. The plant extract was typically added dropwise at a ratio of 1:10 to Cupric nitrate solution in a standard technique (Behera *et al.*, 2012). Following the observation of a colour shift, the resulting mixtures were centrifuged and decanted. The pellet was then rinsed out of the centrifuge tubes using ethanol, which also eliminates contaminants, and dried for two minutes with argon gas before being fully dried in the oven. The blackish colour of the pellets verified the creation of iron oxide nanoparticles, as depicted in Plate 2.0.

Fabrication of M-DSSC

To cover the porous TiO_2 layer, ZrO_2 paste was printed on the TiO_2 layer. The ZrO layer was then prepared by annealing the ZrO_2 paste for 30 minutes at 450°C. (A screen printer fitted with a 70-mesh screen was used for all screen-printing procedures). To prevent contact between the photoanode and the counter electrode, the ZrO_2 paste was printed over the FTO's etched line (Bibi *et al.*, 2019).

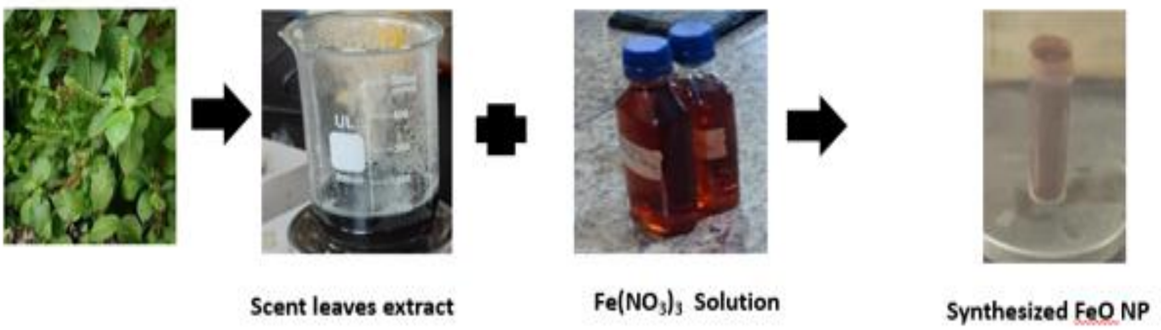

Plate 2.0: Synthesis of FeO nanoparticle

After the substrate cooled, the ZrO_2 layer was printed with carbon conductive paste (Elcocarb solaronix) using doctor blading as the back contact. This was followed by 30 minutes of annealing at 400ºC.

The carbon layer and other FTO layers were joined simultaneously. But for the better counter electrode, which was printed on the ZrO_2 layer after the substrate cooled, carbon conductive paste (Elcocarb solaronix) was put alongside the carbon nanoparticles as back contact by doctor blading, which was then annealed at 400°C for 30 minutes (Bibi et al., 2019)

Monolithic electrodes were made using FTO glass plates (Solaronix). Substrate pre-cleaning involved washing the FTO substrate with propanol and drying it in a spin coater (Labscience model 800) at 3000 RPM. To make mesoporous TiO_2, Ti-Nanoxide was screen printed and then annealed at 450ºC for 30 minutes. The mesoporous films are then treated with a 70 mM solution of $TiCl_4$ at 70°C for 30 minutes, washed with water, and annealed at 500°C for 30 minutes. When the substrate cooled, ZrO_2 paste was applied to the TiO_2 layer to cover the porous TiO_2 layer. The ZrO_2 paste was then annealed at 450ºC for 30 minutes to form a ZrO layer. (All screen-printing steps were carried out with a screen printer equipped with 70 mesh screen). The ZrO_2 paste was made following a described process with ZrO_2 nanoparticles (d=40-50nm; Fulka, USA) (Kuang *et al.*, 2006). When the substrate cooled, carbon conductive paste (Elcocarb solaronix) was placed as back contact by doctor blading, followed by 30 minutes of annealing at 400ºC on the ZrO_2 layer. At the same time, the carbon layer was linked to the remaining FTO layer. The cell stack is immersed overnight in a dye solution containing Chlorin e6 dissolved in Toluene and stored at room temperature (Bibi et al., 2019). The dye-adsorbed photoanode was removed from the solution, washed with toluene, and dried on a hot plate at 60°C in the dark. To combine the dye-coated electrodes with glass plates, a hot-melt glue film was heated to 250ºC for 1min (150µm thick; Bynel 4164, DuPont, USA). While remaining on the hot plate, the temperature is raised to 80ºC, and a drop of the electrolyte solution, a 0.05 M solution of CuI dissolved in acetonitrile, is dropped into a hole drilled into the glass of the constructed cell, forming the completed cell. Finally, the hole was sealed with aluminium foil (0.1mm thick) (Bibi et al., 2019).

Characterization techniques

The nanoparticles' UV-visible absorption spectra were acquired by utilizing a Spectrumlab 752 single-beam UV-vis spectrometer, which functions throughout the 200–800 nm wavelength range at room temperature. The functional groups and component composition of the nanoparticles were investigated using an Agilent Technology Cary 630 FT-IR Spectroscopy. Morphological and elemental composition was carried out using a Field Emission Scanning Electron Microscopy (FE-SEM). X-ray diffraction (XRD) examination was carried out to determine the crystallographic structure. To assess the photovoltaic properties of the cells, the current-voltage characteristics were measured at 100mW/cm^2 using a solar simulator (Newport Oriel, instrument model 65194A-100 solar simulator) connected to a source measure unit, Keithley source meter, Model 2400.

Results and Discussion

Optical absorbance of the synthesized FeO nanoparticle

Figure 1 displays the FeO nanoparticle’s UV–Vis optical absorptions that were synthesized using a fixed ratio of 1:10 of scent leaf and the precursor and samples were collected at different temperatures, ranging from 60ºC to 100ºC. Colour change in the precursor solution confirmed the formation of the nanoparticle (Behera et al., 2012). As the leaf extract and the Iron solution were mixed, the colour changed gradually to brownish black. The dark brown colour became intense as the volume of the extract increased. The resulting intense black-coloured solutions confirmed the synthesis of FeO nanoparticles (Behera et al., 2012). The optical absorptions observed between 350 nm and around 450 nm belong to FeO nanoparticles, as reported in the literature (Balamurughan *et al.*, 2014). The absorbance peaks increased gradually as the temperature of the extract increased up to 100°C. However, the absorbance peak was observed when the extract's temperature was increased to about 70°C. To optimize the concentration required to be incorporated into the DSSC photoanode to fabricate the solar cells, the nanoparticle synthesized with 53.33 g of the precursor at about 70°C was later used for the fabrication of Counter electrodes for the MDSSC.

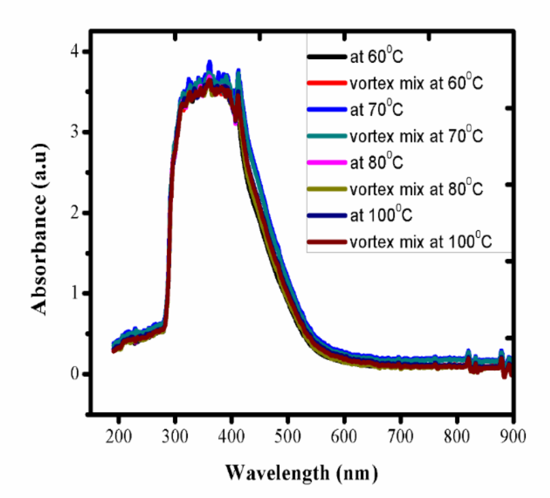

Figure 1: Optical absorbance of the synthesized Nanoparticles

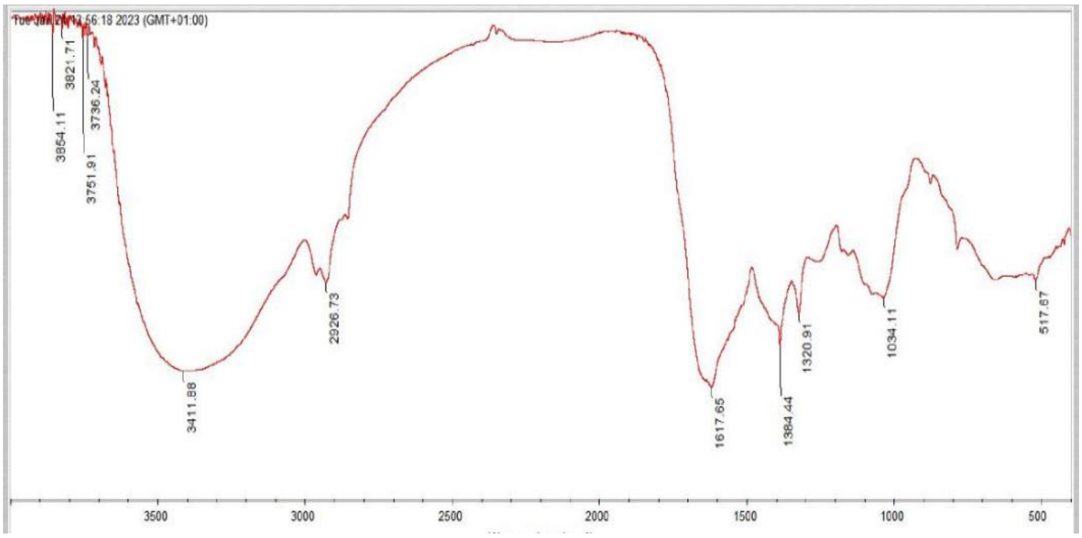

Figure 2: FTIR spectra of the synthesized FeO nanoparticle

FTIR Spectroscopy

Figure 2 shows the FTIR spectra of FeO; a sharp peak was found in the characteristic O-H absorption band with a value of 3411 cm^{-1}. These could be seen in the nanoparticles that were examined. Alkyl C-H stretch is attributed to the organic material in the nanoparticles with a typical absorption range value of 2926 cm^{-1}. At 517 cm^{-1}, FeO_2 showed its distinctive Fe-O vibration bond absorption band these changes are the result of the structural modification brought on by the reaction of the plant extract with the iron oxide.

XRD Studies

The metrics used to assess the crystallinity or amorphous nature of any substance are the sharpness and intensity of the peaks. From Figure 3, FeO nanoparticle is demonstrated by multiple peaks at 2θ around the 200, 220, 332, 333, and 442 planes, respectively, which corresponds to the XRD data for FeO nanoparticles with 2θ values of 13.03°, 18.18°, 29.48°, 33.14°, and 37.50°. The findings point to an efficient nanoparticle with improved crystallinity, as depicted in Figure 3.

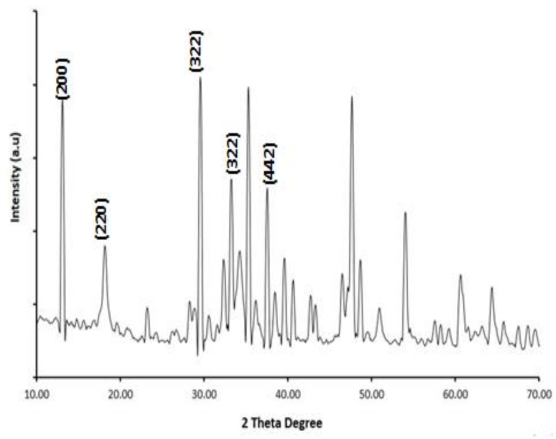

Figure 3: XRD pattern of FeO Nanoparticle

Morphological and compositional studies

The morphologies of the synthesized FeO nanoparticles captured in FE-SEM images in Figure 4. (a-c) are shown at various magnifications. The synthesized FeO has a spherical-like shape and a diameter between one and two microns. A closer inspection reveals that the cross-section of the products shows that the sample is composed of high-yield fibril-like nanostructures with an average length of less than 1 m and a diameter of less than 50 nm. Usually, these fibrils form virtually spherical bundles with widths of 5 µm and an average breadth of about 50 nm. According to Cao *et al.* (2019), these are well shown in Figure 4 (a and b). Iron and other component elements are confirmed to be present by the synthesized nanoparticle's Energy Dispersive Spectral analysis (EDX). Elements like O, Fe, and Tb are visible in the image. The creation of Fe nanoparticles was confirmed by the presence of iron and oxygen. The nature of the extract used to create the nanoparticle may have contributed to the other elements' presence in the nanoparticle.

Photovoltaic performance

These devices' photovoltaic properties are shown in Figure 5 and Table 1. The letters PCE and FF stand for photovoltaic conversion efficiency and fill factor, respectively, of solar cells. The performance of the MDSSC was evaluated by measuring the cell's maximum voltage, maximum current, fill factor, open-circuit voltage, and short-circuit current. Table 1 displays the performance characteristics of FeO (Iron oxide) nanoparticle-free and nanoparticle-containing monolithic Dye-Sensitized Solar Cells (DSSCs). Open-circuit voltage (Voc), short-circuit current density (Jsc), fill factor, voltage at maximum power (Vmp), and current at maximum power (Imp) are among the characteristics that are measured. Table 1 shows that the DSSC without nanoparticles had the lowest solar-to-electric power conversion efficiency of any kind, with 1.7%, an open circuit voltage of 0.2625 V, a short-circuit current of 0.1042 mA/cm^2, a fill factor of 0.46 with solar-to-electric power conversion efficiency of 4.0%. T

This demonstrates that when compared to the cell without nanoparticles, the addition of nanoparticles resulted in a discernible rise in Voc. This implies that these nanoparticles have an impact on the monolithic DSSCs' voltage characteristics. But when the DSSC is short-circuited, the Jsc values, which range from 0.0723 mA/cm^2 to 0.1042 mA/cm^2, show the current output. Notably, FeO showed higher Jsc values in comparison to the nanoparticle-free cell, indicating improved light absorption and electron production. Additionally, greater Vmp and Imp values suggest improved power conversion efficiency. This implies that the counter electrode containing FeO nanoparticles is

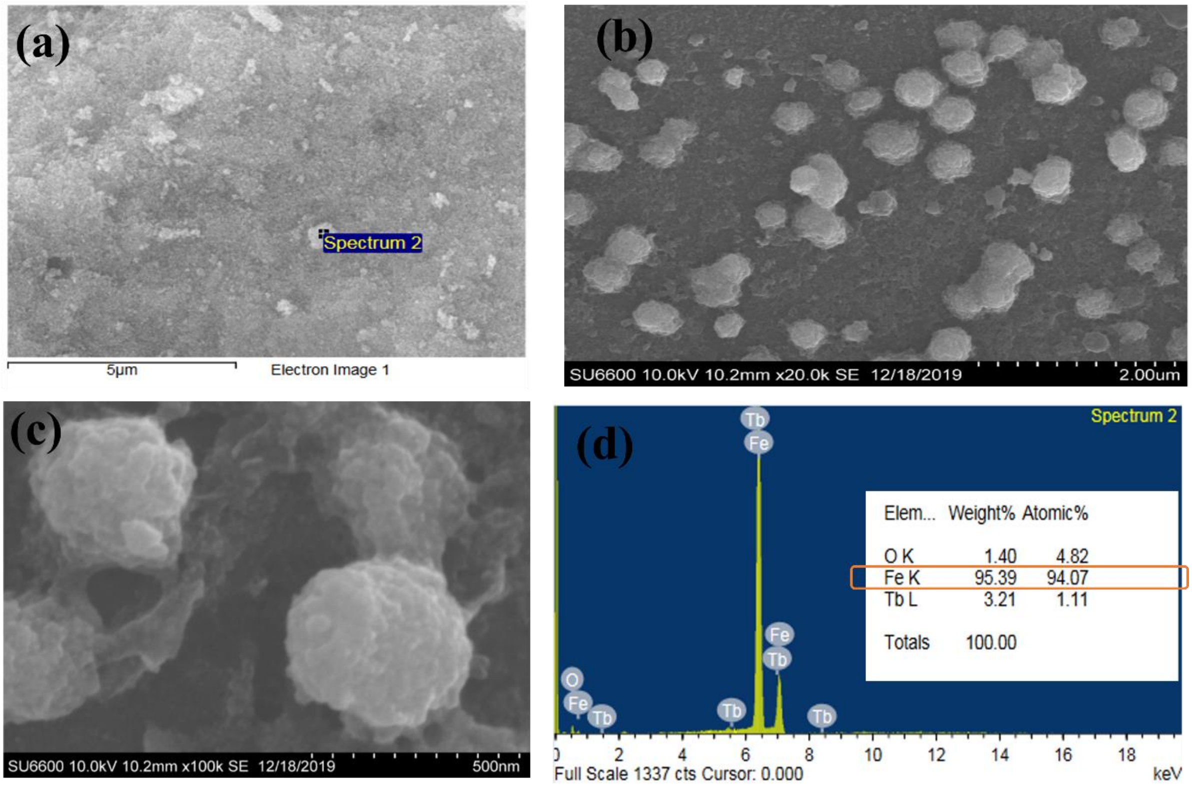

Figure 4: FESEM micrograph and EDX spectral of FeO NP

very useful for promoting the transfer and application of electrical energy produced.

The efficiency of the fill-factor, which indicates how well a solar cell uses the power generated, decreased from 0.46 to 0.36. In this instance, the cells' percentage increase above the cell without nanoparticles indicates that FeO nanoparticles have increased by 135.3%. FeO nanoparticles show the highest efficiency among the investigated compositions, suggesting the synergistic benefits of integrating iron oxide nanoparticles. The total efficiency of the DSSCs is greatly improved with the introduction of nanoparticles. The surface area of the FeO nanoparticles facilitates an electron's rapid migration from the FeO NPs to the TiO_2, which may be the source of the overall increased photovoltaic performance. Collective oscillations can be produced in metals by electrically stimulating free electrons. These oscillations can occur inside a comparatively small volume of a FeO nanoparticle, enhancing the local field and increasing the amount of light incident on the nanoparticles. As a result, the dye-sensitized solar cell's efficiency rose as a result of the iron oxide nanoparticles doped with porous carbon boosting the amount of light absorption.

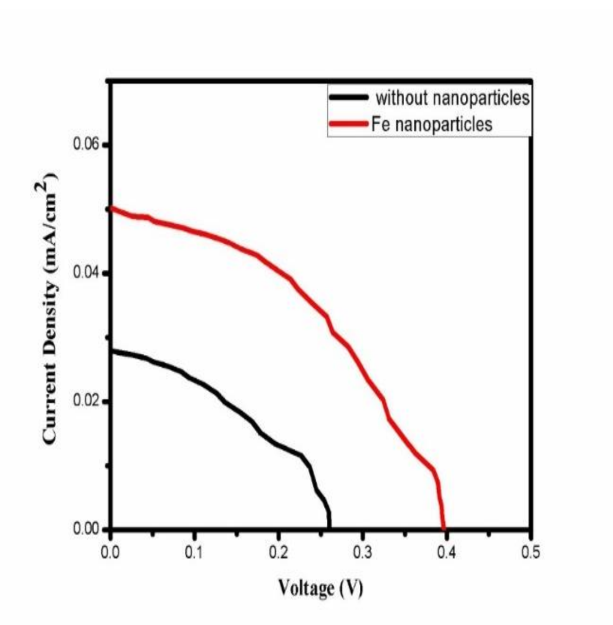

Figure 5: Current Density versus Voltage curves for Monolithic DSSCs

Table 1: Photovoltaic conversion efficiency of Monolithic dye-sensitized solar cells

Nanoparticles	Voc (V)	Jsc (mA/cm^2)	Vmp (V)	Imp (mA/cm^2)	Fill factor	Efficiency (%)
Without NP	0.2650	0.0723	0.1359	0.0508	0.36	1.7
With FeO NP	0.4274	0.1042	0.2626	0.0779	0.46	4.0

The FeO nanoparticles worked as catalysts by increasing the dye absorption of titanium dioxide, and because they are good conductors, this increased the short-circuit current density and increased efficiency. Notably, the open-circuit voltage rose, and the fill factor also became better.

CONCLUSIONS

A unique green production of FeO nanoparticles has been developed utilizing scent leaf extract. The UV-vis was done and showed the absorbance as it increased by adding the plant extract to the precursor. FTIR investigations were done, and the results revealed the presence of several functional groups and their possible role in nanoparticle production. FE-SEM & Edx was done which showed the structure and elemental composition of the nanoparticles. Furthermore, XRD investigations were carried out, and the patterns showed that the synthesized FeO nanoparticle was crystalline in nature with an average crystallite size of 47.9 nm. FeO nanoparticles were incorporated in the fabrication of Monolithic Dye Sensitized Solar Cells with an efficiency of 4.0% obtained for the device prepared by this enhanced counter electrode layer. While 1.7% was achieved for the cell without the nanoparticles. The photo-electrochemical performances using FeO nanoparticles showed a percentage increase in efficiency of 135.3%.

Declaration of Competing Interest The authors declare that none of the work reported in this study could have been influenced by any known competing financial interests or personal relationships.

Data availability Data will be made available on request.

Acknowledgement The authors acknowledge with gratefulness the Pharmaceutical Laboratory, University of Ibadan for the optical characterizations, FTIR characterizations in Bowen University Iwo Osun, Namiroth Nigeria Limited Abuja for the IV characterizations, University Teknologi PETRONAS Malaysia also for XRD and FE-SEM analysis, and members of Nanotechnology Research Group, LAUTECH, Ogbomoso, for their fruitful discussions and technical input.

REFERENCES

Adedokun O., Titilope, K. & Awodugba, A. O. (2016). Review on natural Dye-sensitized solar cells (DSSCs). International Journal of Engineering Technologies, 2: 34-41.

Adedokun, O., Awodele, M. K., Sanusi, Y. K. & Awodugba, A.O. (2018). Natural dye extracts from fruit peels as sensitizers in ZnO-based dye-sensitized solar cells, IOP Conf. Ser. 173, 012040. https://doi.org/10.1088/1755-1315/173/1/012040

Ahmad, R. G. G., Mohammad, M., Hossein, V., Farzad, K., Mahdieh, A. S. R. & Hamed, B. (2019). Fungus-mediated Extracellular

Biosynthesis and Characterization of Zirconium Nanoparticles Using Standard *Penicillium* Species and Their Preliminary Bactericidal Potential: A Novel Biological Approach to Nanoparticle Synthesis. Iranian Journal of Pharmaceutical Research, 18 (4): 2101-2110 https://doi:10.22037/ijpr.2019.112382.13722

Balamurughan, M. G., Mohanraj, S., Kodhaiyolii, S. & Pugalenthi, V. J. (2014). Ocimum sanctum leaf extract mediated green synthesis of iron oxide nanoparticles: spectroscopic and microscopic studies. Chem. Pharm. Sci. 4, 201–204.

Behera, S. S., Patra, J. K., Pramanik, K., Panda, N. & Thatoi, H. (2012). Characterization and evaluation of antibacterial activities of chemically synthesized iron oxide nanoparticles, World J. Nano Sci. Eng. 2, 196 https://doi.org/10.4236/ wjnse.2012.24026

Bibi, I., Nazar, N., Ata, S., Sultan, M., Ali, A., Abbas, A., Jilani, K., Kamal, S., Sarim, F. M., Khan, M. I., Jalal, F. & Iqbal, M. (2019). Green synthesis of iron oxide nanoparticles using pomegranate seeds extract and photocatalytic activity evaluation for the degradation of textile dye, J. Mater. Res. Technol. 8, 6115–6124, https:// doi.org/10.1016/j.jmrt.2019.10.006

Chen, C. Y., Wang, M., Li, J. Y., Pootrakulchote, N., Alibabaei, L., Ngoc-le, C., Decoppet, J. D., Tsai, J. H., GraRtzel, C., Wu, C. G., Zakeeruddin, S. M. & Gratzel, M. (2009). Highly efficient light-harvesting ruthenium sensitizer for thin-film dye-sensitized solar cells, *ACS Nano*, *3*, (10), 3103-3109. https://doi.10.1021/nn900756s

Geoffrey, A. O., Andre, C. A. & Ludovico, C. (2008) Nanochemistry: A chemical approach to Nanomaterials. *RSC Publishing*., *2*, 10-13. https://doi.org/10.1039/9781849737395

Gulzar, A. R., Anima, N., Manzoor, A. P., Showket, Yahya., Mohmmad, A. S., Hamed, B. & Muthupandian, S. (2021). Biosynthesis of Zinc oxide nanoparticles using *Bergenia ciliate* aqueous extract and evaluation of their photocatalytic and antioxidant potential. *Inorganic Chemistry Communications 134, 109020* https://doi.org/10.1016/j.inoche.2021.109020

Cao, D., Yin, H., Yu, X., Zhang, J., Jiao, Y., Zheng, W., Mi, B., and Gao, Z. (2019). Role of modifying photoanodes by organic titanium on charge collection efficiency enhancement in dye-sensitized solar cells. *Advanced Engineering Materials*, 22, 1901071. https://doi.org/10.1002/adem.201901071

Hossein, V., Farzad, K., Ahad, A., Muthupandian, S. & Hamed, B. (2021). Green nanotechnology-based tellurium nanoparticles: Exploration of their antioxidant, antibacterial, antifungal, and cytotoxic potentials against cancerous and normal cells compared to potassium tellurite. *Inorganic Chemistry Communications, 124, 108385* https://doi.org/10.1016/j.inoche.2020.108385.

Hinsch, A., Behrens, S., Berginc, M., Bonnemann, H., Brandt, H., Drewitz, A., Einsele, F., Fasler, D., Gerhard, D., Gores, H., Haag, R., Herzig, T., Himmler, S., Khelashvili, G., Koch, D., Nazmutdinova, G.; Opara-Krasovec, U.; Putyra, P.; Rau, U., Sastrawan, R., Schauer, T., Schreiner, C., Sensfuss, S., Siegers, C., Skupien, K., Wachter, P., Walter, J., Wasserscheid, P., Wurfel, U. & Zistler, M. (2008). Material development for dye solar modules: results from an integrated approach *Prog. Photovolt: Res. Appl. 16*, (6), 489-501

Ito, S., Zakeeruddin S. M. Comete P. Liska P., Kuang D., and Gratzel M. (2008a). Bifacial dye-sensitized solar cells based on an ionic liquid electrolyte, *Nature Photonics*. *2*, 693-698.

Ito, S., Murakami, T.N., Comte, P., Liska, P., Gratzel, C., Nazeeruddin, M. K. & Gratzel, M. (2008b). Fabrication of thin film dye sensitized solar cells with solar to electric power conversion efficiency over 10%, Thin Solid Films 516 (14) 4613–4619. https://doi.org/10.1016/j.tsf.2007.05.090.

Kay, A. & Gratzel, M. (1996). Low-cost photovoltaic modules based on dye sensitized nanocrystalline titanium dioxide and carbon powder *Solar Energy Mater. Solar Cells*, *44*. 99-117. https://doi.org/10.1016/09270248(96)00063-3

Kuang, D., Seigo, I., Bernard, W., Cedric, K., Jacques-E. M., Robin, H., Shaik, Z. & Michael, G. (2006). High molar extinction coefficient heteroleptic ruthenium complexes for thin film dye sensitized solar cells. *Journal of the American Chemical Society*, 12, 4146-4157. https://doi.org/10.1021/ja058540p

Lee, K. S., Kwon, J., Im, J. H., Lee, C. R., Park, N.-G., & Park, J. H. (2012). Size-tunable, fast, and facile synthesis of titanium oxide nanotube powders for dye-sensitized solar cells, ACS Appl. Mater. Interfaces, 4(8), 4164-4168. https://doi.org/10.1021/am300892j

Murakanmi, T. N., Seigo, I., Qing, W., Khaja, N., Takeru, B., Ilkay, C., Paul, L., Robin, H., Pascal, C., & Péter, P. (2006). Highly efficient dye-sensitized solar cells based on carbon black countert electrodes. *Journal of the electrochemical society*, 153 (12) **153** A2255-A2261 https://doi.org/10.1149/1.2358087

O'Regan B., & Gra ̈tzel M. (1991). A low-cost, high-efficiency solar cell based on dye-sensitized colloidal TiO_2 films. Nature 353:737–7404. https://doi.org/10.1038/353737a0

Pandey, S., Oza, G., Mewada, A. & Sharon, M. (2012). Green Synthesis of Highly Stable Gold Nanoparticles using *Momordica charantia* as Nano fabricator. *Arch. Appl. Sci. Res*., *4*,1135-1141.

Park, J. T., Lee, C. S. & Kim, J. H. (2015). High performance electrocatalyst consisting of CoS nanoparticles on an organized mesoporous SnO_2 film: its use as a counter electrode for Pt-free, dye-sensitized solar cells. Nanoscale, 7, 670-678. https://doi.org/10.1039/C4NR05779A

Wang, P., Zakeeruddin, S. M., Comte, P., Exnar, I. & Gratzel, M. *J.* (2003). Gelation of Ionic Liquid-Based Electrolytes with Silica Nanoparticles for Quasi-Solid-State Dye-Sensitized Solar Cells, J. *Am. Chem. Soc*, *125, (5)*, 1166-1167.

https://doi.org/10.1021/ja029294-